MULTIPLE DIPOLAR SOURCES LOCALIZATION FOR MEG USING BAYESIAN PARTICLE FILTERING

Xi Chen, Simon Godsill

Department of Engineering, University of Cambridge, Cambridge, United Kingdom
E-mail: xc253@cam.ac.uk; sjg@eng.cam.ac.uk

ABSTRACT

Electromagnetic source localization is a technique that enables the study of neural dynamical activities on a millisecond timescale using Magnetoencephalography (MEG) or Electroencephalography (EEG) data. It aims to reveal neural activities in the brain cortical region which cannot be seen with imaging methods that operate on a slower timescale such as fMRI. In this paper, we model the problem under a Bayesian multi-target tracking framework. A multi-target detection and particle filtering algorithm is developed to estimate the dipolar source dynamics, and a minimum norm (MN) based estimation method is incorporated to construct the birth-death move for the dynamical number of dipolar sources. The algorithm is tested using both simulated and experimental data[1]. The results demonstrate that the proposed algorithm performs better than that in previous works in terms of both localization accuracy and computational cost.

Index Terms— Localization, dipolar sources, MEG/EEG, Bayesian, particle filter

1. INTRODUCTION

In the past two decades, non-invasive imaging techniques such as functional Magnetic resonance Imaging (fMRI), Magnetoencephalography (MEG) and Electroencephalography (EEG) have been developed to explore the instantaneous activities of the human brain [1]. Amongst these techniques, MEG/EEG have temporal resolutions in millisecond scale, which enables us to observe the electromagnetic source activities in a millisecond range, thereby localizing the active regions in the cortical area.

The MEG/EEG source localization problem is important in clinical applications, such as diagnosing epilepsy, surgical planning and other neuroscience studies [2]. As the electromagnetic signals produced by a single neuron are too weak to be measured, tens of thousands of synchronously neurons are required to produce measurable signals. For the purpose of modeling, many geographically neighboring neurons can be summarized as a "dipole" [1]. Our goal is to localize the brain dipolar sources given MEG data.

There is a significant amount of work modeling the brain currents as dipolar sources, which have addressed the dipole localization problem using various schemes [2, 3, 4, 5, 6]. Some early papers employed optimization techniques [2, 3], whereas others modeled the problem under a Bayesian framework. As the measured data depends nonlinearly on the characteristics of the dipoles, Somersalo et. al. [4] first introduced particle filtering approaches [7] to numerically approximate the dipole characteristics. In [5], a Rao-Blackwellized particle filter was proposed for single/two dipoles tracking. In [6], a random finite sets method was introduced to model the dipole number. However, the performances of these approaches are limited in multi-dipole localization scenarios.

In this paper, we propose a new dipole-based Bayesian particle filtering algorithm. The localization problem is treated as a multi-target tracking problem in a constrained 3D state space—the cortex. A Bayesian particle filtering approach is developed to localize varying numbers of dipoles. The algorithm incorporates a Minimum Norm (MN) estimation method to detect active brain regions before tracking. A nonlinear spherical head model is employed, and a random walk model is used for the state dynamics. The algorithm is tested and compared with those in previous works. Results show that the proposed approach achieves better performance in terms of localization accuracy.

The rest of the paper is organized as follows. Section 2 describes the general problem formulation. Section 3 details the DMAPF algorithm. Section 4 gives results obtained using both simulated and real data. Section 5 makes concluding remarks.

2. PROBLEM FORMULATION

Consider a MEG application with coil sensors $\{s = 1, 2, \cdots, S\}$ distributed outside the surface of the head. Let $\mathbf{X}$ denote an $I \times K$ matrix representing the state of the dipole sources, where $\{k = 1, 2, \cdots, K\}$ denotes the time steps

[1]The author would like to thank CBU MRC of Cambridge Univeristy for providing the datasets, especially Dr.Matti Stenroos for providing suggestions and the Matlab visualization tools, Dr. Rik Henson for putting all data models together and organizing the datasets, Dr. Simo Särkkä and Dr. Olaf Hauk for their useful comments.

978-1-4799-0356-6/13/$31.00 ©2013 IEEE

and $\{i = 1, 2, \cdots, I\}$ indexes the active dipole sources in the cortex. We write $\mathbf{X} = [\mathbf{x}_1 \cdots \mathbf{x}_k \cdots \mathbf{x}_K]$. The state of all dipole sources at time step k is an $I \times 1$ vector $\mathbf{x}_k = [\mathbf{x}_{1,k}^T \cdots \mathbf{x}_{i,k}^T \cdots \mathbf{x}_{I,k}^T]^T$, where $\mathbf{x}_{i,k}$ is a 6×1 vector that describes the features of the ith dipole in a 3D Cartesian coordinate. Specifically, $\mathbf{x}_{i,k} = [\alpha_{i,k}^T, \beta_{i,k}^T]^T$, where $\alpha_{i,k}$ is a location vector and $\beta_{i,k}$ is an amplitude vector (each contain 3 elements). The orientation of a dipolar source can be tangential or radial to the scalp surface (see [1] for details). The magnetic field generated by radial dipoles is very weak compared to that from tangential dipoles. Thus, we assume that the orientation of all simulated dipole sources are fixed as normal to the scalp surface.

Let $\mathbf{Y}$ denote an $S \times K$ matrix representing MEG data measured from the coils, i.e. $\mathbf{Y} = [\mathbf{y}_1 \cdots \mathbf{y}_k \cdots \mathbf{y}_K]$, where $\mathbf{y}_k$ is defined a $S \times 1$ vector $\mathbf{y}_k = [y_{1,k} \cdots y_{s,k} \cdots y_{S,k}]^T$ and $y_{s,k}$ denotes the measurement from sensor s at time step k. The magnetic field $y_{s,k}$ is produced by the neural current density $\mathbf{J}_k(\alpha)$, it can be treated as a sum of several dipolar sources represented by $\mathbf{x}_k$.

We now construct the dipole dynamic model as $\mathbf{x}_{i,k} = f(\mathbf{x}_{i,k-1}, \epsilon_{i,k})$, where ϵ is dynamic noise. The measurement model is defined as $y_{s,k} = b(\mathbf{x}_{i,k}, \zeta_{s,k})$, where ζ is measurement noise.

2.1 Brain dipole modeling

The measurement model is constructed by the Biot-Savart law [1]. We assume that the dipole activities are confined to the cerebral cortex space, which is a 2 - 4 mm thick sheet of gray tissue in the uppermost layer of the brain. The state space is denoted as $\mathbf{\Omega}$, which constrains the dipoles to lie within the cerebral cortex.

Assume we have multiple dipolar sources evloving within $\mathbf{\Omega}$. WE can express the magnetic signal measured by the sth sensor with lead fields that are obtained from forward model. The forward model $b(\mathbf{x}_{i,k}, \zeta_{s,k})$ can be expressed as

$$y_{s,k} = \frac{\mu_0}{4\pi} \int_{\mathbf{\Omega}} \mathbf{J}_k(\alpha) \times \frac{(\mathbf{r}_s - \alpha)}{|\mathbf{r}_s - \alpha|^3} \cdot \mathbf{e}_{\mathbf{r}_s} \mathbf{d}v' + \zeta_{s,k}, \qquad (1)$$

where $\mathbf{r}_s$ is the 3D location of the sth sensor, $\mathbf{e}_i$ is the orientation vector, and $\mu_0 = 4\pi \times 10^{-7}$ is the magnetic permeability electromagnetic constant. More generally, the measurement model is $\mathbf{y}_k = b(\mathbf{x}_k, \zeta_k)$, where we assume the measurement noise $\zeta_{s,k}$ is independent Gaussian with zero mean and variance σ_ζ^2.

In the dipole dynamic model, we assume that the dynamics of dipole sources are independent of each other. We consider a random walk model for dipole state prediction, where the state space is constrained to $\mathbf{\Omega}$. For the ith dipole, we have $\mathbf{x}_{i,k} = \mathbf{x}_{i,k-1} + \epsilon_{i,k}$, where $\epsilon_{i,k}$ is modeled as an independent Gaussian with zero mean and variance σ_ϵ^2. When the sample values exceed the state space $\mathbf{\Omega}$, the algorithm repeats the propagation step until the sample values lie within $\mathbf{\Omega}$.

2.2 Dipole birth-death move

As the number of dipoles evolves over time, an MN-based estimation approach is employed to detect the active cortical regions instantaneously, thus providing information about the number of dipoles. Since the dipole moment varies quickly, we only consider the dipole location $\alpha_{i,k}$ as the criterion for the dipole birth-death move.

At time $k-1$, consider the I_{k-1} dipoles $\{I_{k-1}; \{\alpha_{i,k-1}\}_{i=1}^{I_{k-1}}\}$. MN-based estimation (described in next section) gives $\{\hat{I}_k; \{\hat{\alpha}_{j,k}\}_{j=1}^{\hat{I}_k}\}$ at time k, where $\hat{I}_k$ is the detected dipole number and $\hat{\alpha}_{j,k}$ is the corresponding detected dipole location.

We compute the distance $d_{i,j} = ||\alpha_{i,k-1} - \hat{\alpha}_{j,k}||$. We then introduce $q_{i,j}$ which represents the probability of associating the jth newly detected dipole $\hat{\alpha}_{j,k}$ with the ith dipole at time $k-1$, $q_{i,j} \sim \mathcal{N}(d_{i,j} - d_{thres}, \mathbf{v}_d)$, where d_{thres} is the threshold distance between dipoles, and $\mathbf{v}_d$ is the fixed variance. Thus, we can generate the new dipole number and locations at time k, $\{I_k; \{\alpha_{i,k}\}_{i=1}^{I_k}\}$. For each j, if $q_{i,j} > q_{thres}$, we associate the jth detected dipole with the ith dipole, otherwise it is treated as a new birth. Dipoles at time $k-1$ will be deleted (death) if they are not associated with any detected dipole j, q_{thres} is the fixed value represents the threshold.

3. DMAPF ALGORITHM

Given the above models, the dipole source localization is a nonlinear multi-target tracking problem with a varying number of targets. We now introduce the DMAPF algorithm in two steps: MN-based dipole detection and multiple auxiliary particle filtering.

Step 1. Minimum norm detection

The minimum norm method [8] divides the whole state space into M potential distributed sources with fixed locations, and computes the distributed sources linearly. The $S \times M$ lead field matrix $\mathbf{H}$ was derived with SPM [9] that used the Nolte method [10] as implemented in FieldTrip [11]. We have $\mathbf{y}_k = \mathbf{H}\mathbf{z}_k$. Given $\mathbf{y}_k$ and $\mathbf{H}$, the minimum norm method computes $\hat{\mathbf{z}}_k$, which contains M elements describing the moment for each of the distributed sources. Elements in $\hat{\mathbf{z}}_k$ with large fluctuations will then be identified; an agglomerative clustering algorithm [12] is applied to construct clusters of potential sources. Consequently, the clustered sources are provided as newly detected dipoles $\{\hat{I}_k; \{\hat{\alpha}_{j,k}\}_{j=1}^{\hat{I}_k}\}$ for the birth-death move. In practice, as most dipoles exist for several time steps, the minimum norm detection is executed every L particle filtering runs, i.e. every L time steps.

Step 2. Multi-target particle filtering

During every L time steps, the problem appears as a multi-dipole tracking problem with a fixed number of dipoles. Here we introduce a multiple particle filtering concept, which was first developed in [13]. The basic idea is to assign each target an individual Particle Filter (iPF). Each iPF updates new target estimates based on estimations given by the rest of the iPFs. At each time k, iPFs cooperate with each other and the multiple particle filter operates in a sequential manner. This particle filtering algorithm is an approximate procedure that substitutes posterior mean estimates for other targets.

To fit the dipole localization problem, the posterior density function (pdf) can be written as $p(\mathbf{x}_{i,0:k}|\mathbf{y}_{1:k}, \mathbf{x}_{-i,0:k})$, where $\mathbf{x}_{-i,0:k}$ is the state vector excluding $\mathbf{x}_{i,0:k}$.

The observed dipole dynamic implies that the dipole state $\mathbf{x}_k$ may vary significantly from its previous time step. This results in a high variance of weights when we perform sequential sampling importance resampling (SIR) [7]. In contrast with the algorithm developed in [13] which uses a SIR filter, we incorporate an auxiliary particle filter [14].

The algorithm first propagates N particle samples for each dipole (or each iPF). Particles evolve according to the dynamic model $p(\mathbf{x}_{i,k}|\mathbf{x}_{i,k-1}^{(n)})$. The algorithm then assign a weight for each particle sample. The unnormalized weight equation is $\omega_{i,k} = \frac{p(\mathbf{x}_{i,k}|\mathbf{y}_k,\mathbf{x}_{-i,k})}{\pi(\mathbf{x}_{i,k}|\mathbf{y}_k,\mathbf{x}_{-i,k})}$, where $\pi(\mathbf{x}_{i,0:k}|\mathbf{y}_{1:k}, \mathbf{x}_{-i,0:k})$ is an appropriately chosen importance distribution.

Algorithm 1: DMAPF Algorithm

```
// Initialization at time step k=0
```
for $i = 1, \ldots, I_k$ *and* $n = 1, \ldots, N$ **do**
  Sample: $\mathbf{x}_{i,0}^{(n)} \sim p_{\mathbf{\Omega}}(\mathbf{x}_{i,0})$, assign weight:
  $\omega_{i,0}^{(n)} = \frac{1}{N}$, estimate: $\hat{\mathbf{x}}_{i,0} = \sum_{n=1}^{N} \omega_{i,0}^{(n)} \mathbf{x}_{i,0}^{(n)}$;
```
// Filtering when k>0
```
for $k = 1, \ldots, K$ **do**
  for $i = 1, \ldots, I_k$ **do**
    for $n = 1, \ldots, N$ **do**
      Sample: $\mathbf{x}_{i,k}^{(n)} \sim p(\mathbf{x}_{i,k}|\mathbf{x}_{i,k-1}^{(n)}, \hat{\mathbf{x}}_{-i,k-1})$;
    predict: $\tilde{\mathbf{x}}_{i,k} = \sum_{n=1}^{N} \omega_{i,k-1}^{(n)} \mathbf{x}_{i,k}^{(n)}$;
  for $i = 1, \ldots, I_k$ **do**
    for $n = 1, \ldots, N$ **do**
```
      // First-stage weights
```
      Assign: $\omega_{i,k}^{(n)} \propto \omega_{i,k-1}^{(n)} p(\mathbf{y}_k|\mathbf{x}_{i,k}^{(n)}, \tilde{\mathbf{x}}_{-i,k})$ and normalize.
```
    // Resampling
```
    $\{\mathbf{x}_{i,k}^{(n)}, \omega_{i,k}^{(n)}\}_{n=1}^{N}$ to $\{\mathbf{x}_{i,k}^{(n^m)}, \frac{1}{N}, n^m\}_{m=1}^{N}$;
    for $m = 1, \ldots, N$ **do**
      Sample: $\mathbf{x}_{i,k}^{(m)} \sim p(\mathbf{x}_{i,k}|\mathbf{x}_{i,k-1}^{(n^m)}, \hat{\mathbf{x}}_{-i,k-1})$;
```
      // Second-stage weights
```
      Assign: $\omega_{i,k}^{(m)} \propto \frac{p(\mathbf{y}_k|\mathbf{x}_{i,k}^{(m)},\tilde{\mathbf{x}}_{-i,k})}{p(\mathbf{y}_k|\mathbf{x}_{i,k}^{(n^m)},\tilde{\mathbf{x}}_{-i,k})}$ and normalize.
  for $i = 1, \ldots, I_k$ **do**
    $\hat{\mathbf{x}}_{i,k} = \sum_{m=1}^{N} \omega_{i,k}^{(m)} \mathbf{x}_{i,k}^{(m)}$;
```
  // MN-based detection
```
  if $k \mod L == 0$ **then**
    Generate $\{\hat{I}_k; \{\hat{\alpha}_{j,k}\}_{j=1}^{\hat{I}_k}\}$ from $\hat{\mathbf{z}}_k$;
    Derive new $\{I_k; \{\alpha_{i,k}\}_{i=1}^{I_k}\}$.

The algorithm is described in Algorithm 1. It contains two weight calculation stages. The *first-stage weight* is derived similarly to SIR [7]. With an appropriate choice of the importance density $\pi(.)$, we have

$$\omega_{i,k}^{(n)} \propto \omega_{i,k-1}^{(n)} \frac{p(\mathbf{y}_k|\mathbf{x}_{i,k}^{(n)}, \mathbf{x}_{-i,k}) p(\mathbf{x}_{i,k}|\mathbf{x}_{i,k-1}^{(n)}, \mathbf{x}_{-i,k-1})}{\pi(\mathbf{x}_{i,k}|\mathbf{x}_{i,k-1}^{(n)}, \mathbf{y}_k, \mathbf{x}_{-i,k-1})}, \quad (2)$$

and choosing the prior as the importance density distribution gives $\omega_{i,k}^{(n)} \propto \omega_{i,k-1}^{(n)} p(\mathbf{y}_k|\mathbf{x}_{i,k}^{(n)}, \mathbf{x}_{-i,k})$.

This expression needs to incorporate an estimate of $\mathbf{x}_{-i,k}$ when drawing samples and assigning weights, respectively. We compute the estimates from samples of each iPF and the *prediction* state at time k is chosen as the mean estimate $\sum_{n=1}^{N} \omega_{i,k-1}^{(n)} \mathbf{x}_{i,k}^{(n)}$. Once new weights are obtained at time k, we compute the *estimation* state as: $\hat{\mathbf{x}}_{i,k} = \sum_{n=1}^{N} \omega_{i,k}^{(n)} \mathbf{x}_{i,k}^{(n)}$.

An auxiliary variable n^m is introduced to aid during the resampling step, which gives $\mathbf{x}_{i,k}^{(n^m)}$; it refers to the index of the samples after resampling. The new samples $\mathbf{x}_{i,k}^{(m)}$ are then propagated according to the dynamic density distribution $p(\mathbf{x}_{i,k}|\mathbf{x}_{i,k-1}^{(n^m)}, \mathbf{x}_{-i,k-1})$. The second-stage weight is obtained as a minor modification to the standard auxiliary particle filter weight: $\omega_{i,k}^{(m)} \propto \frac{p(\mathbf{y}_k|\mathbf{x}_{i,k}^{(m)},\mathbf{x}_{-i,k})}{p(\mathbf{y}_k|\mathbf{x}_{i,k}^{(n^m)},\mathbf{x}_{-i,k})}$.

4. NUMERICAL RESULTS

Here we present numerical results using both simulated and real MEG data.

4.1 Simulated data

We simulate single/two/dynamical four dipoles cases. There are 102 magnetometers distributed close to the surface of the head. The state space $\mathbf{\Omega}$ is confined to the outer layer of the head model with 15 length units thickness. The width of the brain is about 136 length units. We assume the evolution for dipole location/amplitude are independent and identical on each axis of the coordinate, respectively. The orientation vector $\mathbf{e}$ is set to be fixed and perpendicular to the brain surface. The standard deviation of the measurement noise equals 80% of the mean ground-truth noiseless signal. The ground-truth step length of the dipole location is set less than 30 length units and the dipole amplitude is set as 20 length units.

We run the algorithm 30 times for each simulation to generate the root mean square error (RMSE). The algorithm assigns iPFs for each of the I_k dipoles. Each iPF has 500 particles, i.e., $500 \times I_k$ particles at time k. Although a more accurate estimation can be obtained if more particles are assigned for each iPF, the computational cost will greatly increase. This setting provides a good balance between the algorithmic stability and computational efficiency. Visualizations were carried out with tools further developed from those published in Helsinki BEM Library [15].

A. Single/Two dipoles

We generate the MEG data for 20 time steps. For the high noise level case, the location noise variance $\rho_{i,k}^2$ is initialized as 15^2, and the amplitude variance $\eta_{i,k}^2$ is set as 10^2. For the low noise level case, $\rho_{i,k}^2$ equals 10^2 and $\eta_{i,k}^2$ is set as 7.5^2. At time $k = 0$, we initialize the particle location by drawing samples from an uniform distribution over the whole constrained volume $\mathbf{\Omega}$, and the particle amplitude by drawing samples from an uniform distribution $\mathcal{U} \sim (5, 25)$. For single dipole simulation, the RMSE over 30 realizations are shown in Table 1. Under a same noise setting, we compare the DMAPF with an SIR filter in [4]. As the MN-based detection provides us raw information of dipole locations, the tracking accuracy of DMAPF is better than that of SIR. A two dipoles simulation result is shown in Figure 1, we plot both location/amplitude errorbar over 30 realizations for one of the two dipoles.

/Length unit	Loc/x	Amp/x	Loc/y	Amp/y	Loc/z	Amp/z
DMAPF(H)	11.22	10.76	11.08	10.90	12.31	12.55
SIR(H)	16.83	17.95	16.32	16.37	16.98	17.42
DMAPF(L)	8.92	8.10	8.16	8.59	10.01	10.26
SIR(L)	12.22	13.37	12.33	13.76	12.95	13.13

Table 1. RMSE of two algorithms for a single dipole tracking, H/L: high/low noise level, Loc/Amp: Location/Amplitude, x/y/z: the 3D coordinate.

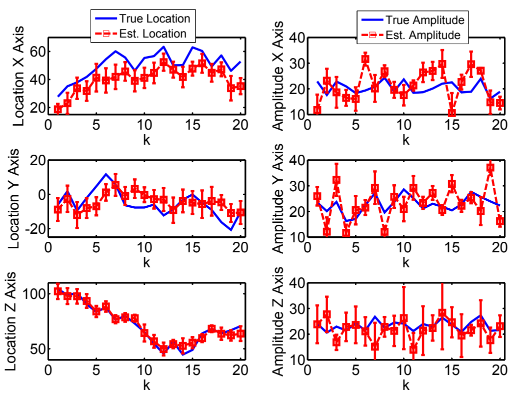

Fig. 1. Dipole location and amplitude error bar of dipole B in a two dipoles tracking

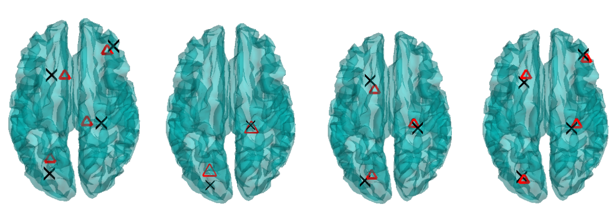

(a) k=1 (b) k=15 (c) k=22 (d) k=35

Fig. 2. Dynamical number of dipoles tracking. Black cross: ground-truth location / Red triangle: estimated location.

B. Four/Dynamical dipoles

We simulate the dynamical dipoles scenario for 50 time steps, i.e., 10 MN-based detection runs. Up to 4 dipoles can appear simultaneously, dipoles may disappear at some k to mimic the dynamics of the dipole numbers. As shown in Figure 2, we plot results at time $k = 1, 15, 22, 35$ with the ground-truth dipole number is 4,2,3,4, respectively. The estimation in $k = 35$ is much better than that in $k = 1$ as the particle filter obtained more data. It is difficult to show the amplitude estimates in the graph, the amplitude RMSE is similar to that in Table 1.

The k-means clustering [16] used in [6] needs to specify a fixed number of clusters before implementing, which constrains the localization performance. DMAPF algorithm addresses the problem by applying the agglomerative clustering, which classifies data with a dynamical number of clusters.

4.2 Real data

We also test the algorithm using a set of real MEG data. The data were sampled at 1KHz, through a lowpass filter to 40Hz. An auditory stimulus appeared at both left and right side of the subjects. The data were epoched from -100ms and recorded until +400ms, and were averaged over at least 100 events under the same setting. As shown in Figure 3, the estimations of both DMAPF and a standard Minimum Norm Estimation (MNE) [8] are ploted in the same figures. The coloured area is the scaled plot from MNE, the colour bars on the right represents the strength of the MNE inverse solution in brain cortex. We plot results at time +240ms, +260ms and +300ms; each detected 4, 3, and 4 dipoles, respectively.

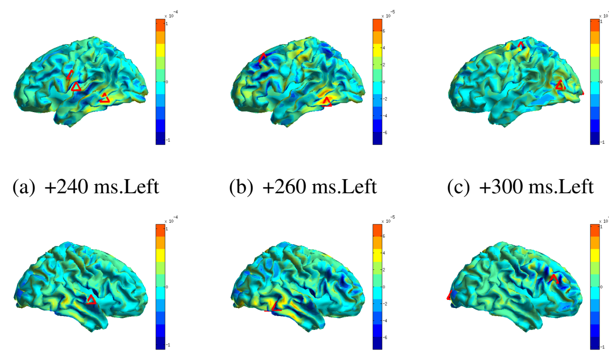

(a) +240 ms.Left (b) +260 ms.Left (c) +300 ms.Left

(d) +240 ms.Right (e) +260 ms.Right (f) +300 ms.Right

Fig. 3. DMAPF and MNE comparision in real MEG data, upper/lower rows show right/left hemisphere respectively. The red triangle denotes the estimated location, the colorbar shows the amplitude of MNE estimates.

5. CONCLUSION

This paper proposed a joint detection and particle filtering approach for MEG multiple dipolar sources localization problem. The algorithm is tested and compared with previous algorithm in both simulated and real data. The results demonstrate that the proposed algorithm improves the multi-dipole tracking performance.

References

[1] M. Hämäläinen, R. Hari, R.J. Ilmoniemi, J. Knuutila, and O.V. Lounasmaa, "Magnetoencephalography: Theory, instrumentation, and applications to noninvasive studies of the working human brain," *Reviews of modern Physics*, vol. 65, no. 2, pp. 413–497, 1993.

[2] J.C. Mosher and R.M. Leahy, "Recursive MUSIC: a framework for EEG and MEG source localization," *IEEE Trans. on Biomedical Engineering*, vol. 45, no. 11, pp. 1342–1354, 1998.

[3] K. Uutela, M. Hamalainen, and R. Salmelin, "Global optimization in the localization of neuromagnetic sources," *IEEE Trans. on Biomedical Engineering*, vol. 45, no. 6, pp. 716–723, 1998.

[4] E. Somersalo, A. Voutilainen, and J.P. Kaipio, "Nonstationary magnetoencephalography by Bayesian filtering of dipole models," *Inverse Problems*, vol. 19, pp. 1047–1063, 2003.

[5] C. Campi, A. Pascarella, A. Sorrentino, and M. Piana, "A Rao–Blackwellized particle filter for magnetoencephalography," *Inverse Problems*, vol. 24, no. 2, pp. 23–37, 2008.

[6] A. Sorrentino, L. Parkkonen, A. Pascarella, C. Campi, and M. Piana, "Dynamical MEG source modeling with multi-target Bayesian filtering," *Human Brain Mapping*, vol. 30, no. 6, pp. 1911–1921, 2009.

[7] A. Doucet, S. Godsill, and C. Andrieu, "On sequential Monte Carlo sampling methods for Bayesian filtering," *Statistics and Computing*, vol. 10, no. 3, pp. 197–208, 2000.

[8] O. Hauk, "Keep it simple: a case for using classical minimum norm estimation in the analysis of eeg and meg data," *Neuroimage*, vol. 21, no. 4, pp. 1612–1621, 2004.

[9] K.J. Friston, A.P. Holmes, K.J. Worsley, J.P. Poline, C.D. Frith, and R.S.J. Frackowiak, "Statistical parametric maps in functional imaging: a general linear approach," *Human brain mapping*, vol. 2, no. 4, pp. 189–210, 1994.

[10] G. Nolte, "The magnetic lead field theorem in the quasistatic approximation and its use for magnetoencephalography forward calculation in realistic volume conductors," *Physics in Medicine and Biology*, vol. 48, no. 22, pp. 3637 – 3652, 2003.

[11] R. Oostenveld, P. Fries, E. Maris, and J. Schoffelen, "Fieldtrip: open source software for advanced analysis of meg, eeg, and invasive electrophysiological data," *Computational intelligence and neuroscience*, vol. 2011, pp. 1, 2011.

[12] K.C. Gowda and G. Krishnan, "Agglomerative clustering using the concept of mutual nearest neighbourhood," *Pattern Recognition*, vol. 10, no. 2, pp. 105–112, 1978.

[13] M.F. Bugallo, T. Lu, and P.M. Djuric, "Target tracking by multiple particle filtering," in *Proc. IEEE Aerospace Conf.*, 2007, pp. 1–7.

[14] M.K. Pitt and N. Shephard, "Filtering via simulation: Auxiliary particle filters," *Journal of the American Statistical Association*, vol. 94, no. 446, pp. 590–599, Jun. 1999.

[15] M Stenroos, V Mäntynen, and J Nenonen, "A matlab library for solving quasi-static volume conduction problems using the boundary element method," *Computer methods and programs in biomedicine*, vol. 88, no. 3, pp. 256–263, 2007.

[16] J.A. Hartigan and M.A. Wong, "Algorithm as 136: A k-means clustering algorithm," *Journal of the Royal Statistical Society. Series C (Applied Statistics)*, vol. 28, no. 1, pp. 100–108, 1979.